

Appl1 and *Appl2* are Expendable for Mouse Development But Are Essential for HGF-Induced Akt Activation and Migration in Mouse Embryonic Fibroblasts

YINFEI TAN,^{1*} XIAOBAN XIN,² FRANCIS J. COFFEY,³ DAVID L. WIEST,³ LILY Q. DONG,² AND JOSEPH R. TESTA^{1*}

¹Cancer Biology Program, Fox Chase Cancer Center, Philadelphia, Pennsylvania

²Department of Cellular and Structural Biology, University of Texas Health Science Center at San Antonio, San Antonio, Texas

³Blood Cell Development and Function Program, Fox Chase Cancer Center, Philadelphia, Pennsylvania

Although *Appl1* and *Appl2* have been implicated in multiple cellular activities, we and others have found that *Appl1* is dispensable for mouse embryonic development, suggesting that *Appl2* can substitute for *Appl1* during development. To address this possibility, we generated conditionally targeted *Appl2* mice. We found that ubiquitous *Appl2* knockout (*Appl2*^{-/-}) mice, much like *Appl1*^{-/-} mice, are viable and grow normally to adulthood. Intriguingly, when *Appl1*^{-/-} mice were crossed with *Appl2*^{-/-} mice, we found that homozygous *Appl1*;*Appl2* double knockout (DKO) animals are also viable and grossly normal with regard to reproductive potential and postnatal growth. *Appl2*-null and DKO mice were found to exhibit altered red blood cell physiology, with erythrocytes from these mice generally being larger and having a more irregular shape than erythrocytes from wild type mice. Although *Appl1/2* proteins have been previously shown to have a very strong interaction with phosphatidylinositol-3 kinase (Pi3k) in thymic T cells, Pi3k-Akt signaling and cellular differentiation was unaltered in thymocytes from *Appl1*;*Appl2* (DKO) mice. However, *Appl1/2*-null mouse embryonic fibroblasts exhibited defects in HGF-induced Akt activation, migration, and invasion. Taken together, these data suggest that *Appl1* and *Appl2* are required for robust HGF cell signaling but are dispensable for embryonic development and reproduction.

J. Cell. Physiol. 231: 1142–1150, 2016. © 2015 Wiley Periodicals, Inc.

APPL1 was discovered as a binding partner to AKT2 and PI3K p110 β by use of a yeast two-hybrid assay (Mitsuuchi et al., 1999). Over the past 15 years, both APPL1 and the subsequently identified APPL2 (Miaczynska et al., 2004; Lin et al., 2006; Mao et al., 2006; Ryu et al., 2014) were found to bind to and regulate many other signaling proteins such as Rab5, GIPC, adiponectin receptors, insulin receptor, and IRS1/2 to affect cell proliferation, migration and metabolism (Miaczynska et al., 2004; Lin et al., 2006; Mao et al., 2006; Ryu et al., 2014). Our group also discovered that murine *Appl1* and *Appl2* both bind to the p110 subunit of phosphatidylinositol-3 kinase (Pi3k), with the strongest interaction documented in thymic T cells (Tan et al., 2010a).

A role for AKT2 in glucose metabolism was first proposed in 1998, when murine *Akt2* was found to be highly expressed in embryonic brown fat and its kinase product was shown to be robustly activated by insulin (Altomare et al., 1998). Subsequent work revealed that an interaction between AKT and APPL1 was required for insulin-stimulated Glut4 translocation and to promote insulin secretion in pancreatic beta cells (Saito et al., 2007; Cheng et al., 2012; Wang et al., 2013). However, the influence of *Appl1/2* proteins on Akt activation appears to be highly context dependent. Specifically, some reports indicate that *Appl* proteins facilitate Akt activation during insulin signaling or during phagocytosis (Saito et al., 2007; Yeo et al., 2015). Other groups have reported converse findings, with *Appl* impairing cell migration and osteoclastogenesis by suppressing AKT (Tu et al., 2011; Broussard et al., 2012). In muscle cells, APPL2 can act as a negative regulator of adiponectin and insulin signaling by competing with APPL1 in the binding of adiponectin receptors

and by sequestering APPL1 from these two pathways (Wang et al., 2009). In contrast, *Appl2* is required for Akt activation during phagocytosis of macrophages (Yeo et al., 2015).

In addition to their roles in insulin and adiponectin signaling, APPL proteins have been implicated in endocytosis. APPL proteins are enriched at the membrane of early endosomes and participate in cell trafficking via binding to RAB5 and RAB21 (Miaczynska et al., 2004; Zhu et al., 2007). Mutation of the inositol

Conflict of interest: The authors have no potential conflicts of interest to disclose.

Contract grant sponsor: NIH;

Contract grant numbers: NCI-CA77429, CA083638, CA06927, NIDDK-DK102965.

Contract grant sponsor: American Diabetes Association;

Contract grant number: 7-13-B5-043.

Contract grant sponsor: Commonwealth of Pennsylvania.

Contract grant sponsor: Fox Chase Cancer Center.

*Correspondence to: Yinfei Tan and Joseph R. Testa, Cancer Biology Program, Fox Chase Cancer Center, 333 Cottman Avenue, Philadelphia, PA 19111. E-mail: yinfei.tan@fccc.edu (Y.T.) and Joseph.Testa@fccc.edu (J.R.T.)

Manuscript Received: 6 August 2015

Manuscript Accepted: 5 October 2015

Accepted manuscript online in Wiley Online Library (wileyonlinelibrary.com): 7 October 2015.

DOI: 10.1002/jcp.25211

5-phosphatase OCRL, which causes Lowe syndrome, abolishes the interaction between APPL1 and OCRL, causing trafficking failure in early endosomes (Erdmann et al., 2007). Adding even more complexity to APPL protein function, both APPL1 and APPL2 have been found to promote the survival of pancreatic cancer cells after radiation via ATM-mediated DNA repair (Hennig et al., 2014). APPL1 can also be recruited to ubiquitin-rich aggresomes in response to proteasome inhibition, which has been proposed to regulate aggresome function (Pilecka et al., 2011).

The overall complexity of the in vitro data is partially supported by in vivo knockdown studies. In lower vertebrate models, *App11* knockdown induces neural cell death during the embryonic development of zebrafish or triggers apoptosis of pancreas and stomach progenitor cells in *Xenopus* (Schenck et al., 2008; Wen et al., 2010). To validate the results of mRNA knockdown studies and exclude off-target effects commonly seen in such experiments, knockout mouse models of *App11* and *App12* should be carefully evaluated. We previously discovered that *App11* is not essential in mammals, as *App11* $-/-$ knockout mice were found to be viable and phenotypically normal (Ryu et al., 2014; Tan et al., 2010a,b), which has been confirmed by others (Cheng et al., 2012; Ryu et al., 2014). Homozygous *App11* knockout mice showed no obvious defects during embryonic development, postnatal growth and reproduction. Moreover, in vivo Pi3k-Akt signaling was not impaired (Tan et al., 2010a). This poses an intriguing possibility that *App11* and *App12* may have overlapping functions, such that *App12* alone is sufficient to compensate for *App11* loss. To test this hypothesis, we generated *App12* knockout mice, which were subsequently crossed with *App11*-null mice. Like *App11*-null mice, *App12*-null mice do not manifest obvious defects in embryonic development or postnatal growth. Moreover, much to our surprise, *App11;App12* double knockout (DKO) mice were also found to be viable and fertile. Mice of different genotypes were born at expected Mendelian ratios, and litter size was normal in the DKO mice. Moreover, T cells from the DKO showed normal Pi3k-Akt signaling and normal development of the thymus. However, murine embryonic fibroblasts (MEFs) from *App11;App12* DKO mice exhibited defects in HGF-induced Akt activation, migration and invasion, providing further support for a context-dependent role of *App11/2* proteins in Akt activation.

Materials and Methods

Generation of conditional *App12* knockout and *App11;App12* double knockout mice

Exon 5 of the *App12* gene was flanked by two *LoxP* sites using conventional gene targeting strategies. In short, one *LoxP* sequence was inserted into Intron 4 of *App12*, and a *Frt-Neo-Frt-LoxP* sequence was inserted into Intron 5. The targeting construct was transfected into ES cells, and correctly targeted ES cell clones were used to generate chimeric mice. Southern blotting was carried out to identify mice with the correctly targeted allele. *App12* floxed mice were mated with EIIA-Cre mice to generate ubiquitous *App12* knockout mice. PCR conditions and the primer sequences for genotyping of the pre- or post-Cre *App12*-allele are listed in Table 1. Next, the *App12* $-/-$ mice were crossed with previously reported *App11* $-/-$ mice (Tan et al., 2010b) to generate *App11;App12* DKO mice.

Reagents

Antibodies against *App11*, total and phospho-Akt, phospho-AMPK, total and phospho-Erk, p38, cleaved caspase3, and Parp were from Cell Signaling (Danvers, MA). Antibodies against β -actin, QM, and GAPDH were from Santa Cruz Biotechnology (Dallas, TX). *App12* antibody was generated by one of us (LQD). EGF and HGF were purchased from R&D Systems (Minneapolis, MN). Tunicamycin and camptothecin were from Selleckchem (Houston, TX).

TABLE 1. Genotyping primers for *App12* targeted allele

Primer name	Sequence
Single <i>Lox P</i> site	
F	TTCTCTCAGAAGAAAGTTGC
R	ATCCTCATTTGACTCAAGGC
Neo cassette	
F	GCACTGTTCCTGAGAAGG
R	TTGGCTGGACGTAAACTCC
<i>App12</i> knockout	
F	ACAGGGTACTGGTACTCATGC
R	ACTGTGCTCACAGGTGTACC
WT	
F	GCACTGTTCCTGAGAAGG
R	ACTGTGCTCACAGGTGTACC

F, forward; R, reverse; WT, wild type.

Complete blood count (CBC) and flow cytometry analysis

Mouse blood was drawn retro-orbitally and measured by VetScan HM5 (Abaxis, Union City, CA). In brief, about 50 μ l of peripheral blood was collected into an EDTA-coated 0.5 ml tube (BD, San Jose CA), and CBCs were assessed within 1 h.

Flow cytometry was performed with a BD LSRII machine to analyze T cell developmental markers. Anti-CD4-APC/Cy7, anti-CD8-PE, anti-CD44-APC/Cy7, and anti-CD25-PE were obtained from BioLegend (San Diego, CA). Data were analyzed by using FlowJo software.

Cell cycle analysis

Cells were fixed with 70% ice-cold ethanol for 2 h at 4°C, washed twice with ice-cold PBS, and then stained with propidium iodine solution for 20 min. Samples were subjected to FACScan (Beckman, Brea, CA) analysis using FlowJo software.

Mouse embryonic fibroblast culture and treatment

E13.5-day embryos from wild type (WT), *App11* KO, *App12* KO, and *App11;App12* DKO mice were collected. Each carcass, minus organs and head, was subjected to 0.2% collagenase for 30 min at 37°C. Isolated cells were washed twice with DMEM supplemented with 10% FBS and 2 mM L-glutamine. Cells were seeded at 1×10^5 /well in a 6-well plate overnight, starved in serum-free media for 1 h, followed by stimulation with 20 ng/ml EGF, 10% FBS, or 50 ng/ml HGF for the indicated times.

Migration and invasion assays

To evaluate cell migration, a Transwell migration assay was used in which 2×10^4 cells were resuspended in 0.1% DMEM and then seeded on a 8.0- μ M PET insert (Corning, Oneonta, NY). Inserts were placed in a 24-well plate with DMEM containing 100 ng/ml HGF and 0.1% FBS in the bottom chamber. After 6 h, inserts were fixed and stained. Cells that migrated through the membrane were photographed and counted. For the invasion assay, a growth factor-reduced Matrigel invasion chamber (Corning) was used, and cells were counted 48 h after seeding. For the wound-healing assay, each well with confluent cells was scratched with a pipette tip, and the rate for the closure of the gap was monitored.

Results

Targeted knockout of *App12* in mice

To facilitate studies of either whole-body or tissue-specific roles of *App12*, we conditionally targeted the mouse *App12* gene. Exon 5 of the mouse *App12* gene was flanked by two *LoxP* sites (Fig. 1A). Southern blot analysis was performed to identify mice with homozygously floxed *App12* (*App12*^{L/L}) alleles

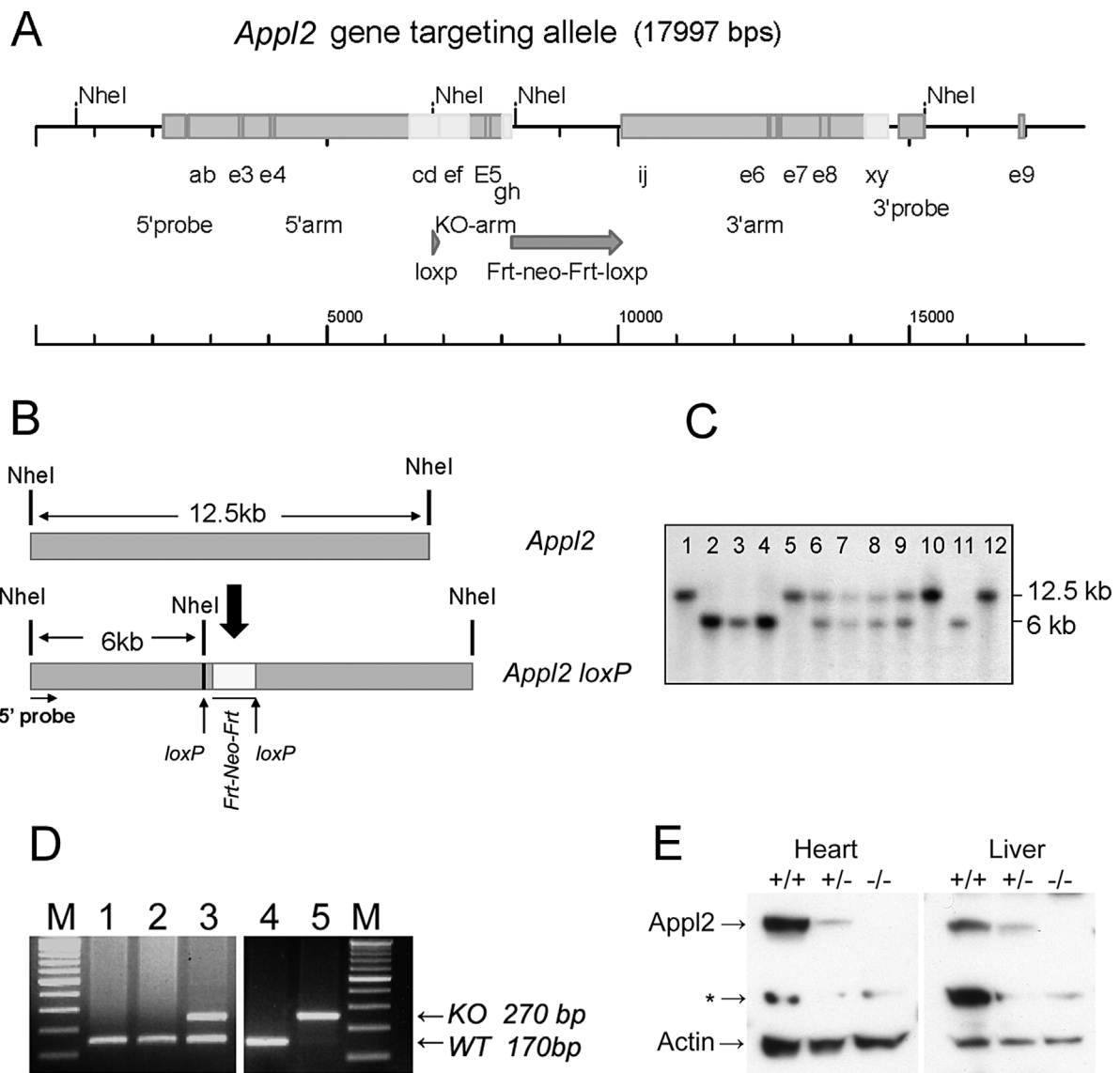


Fig. 1. Conditional targeting of mouse *Appl2* gene. Diagram depicting insertion of *LoxP* sites in Intron 4 and Intron 6 (A). Restriction endonuclease map (B) and Southern blot analysis (C) performed to identify mice with floxed *Appl2* allele(s). Mice represented by lanes 6, 7, 8, and 9 are heterozygous (*Appl2*^{+/L}), whereas those depicted in lanes 2, 3, 4, and 11 are homozygous (*Appl2*^{L/L}). *Appl2* floxed mice were crossed to *EIIA-Cre* mice to obtain whole-body excision of the *Appl2* gene. Genotyping performed by PCR on tail DNA signify wild type (lanes 1, 2, and 4), heterozygous (lane 3) and homozygous *Appl2* knockout alleles (lane 5; D). Immunoblot analysis demonstrating loss of *Appl2* protein expression in heart and liver tissues of *Appl2*^{-/-} mice (E). *, nonspecific band.

(Fig. 1B and C). To address the question about whether *Appl2* is required for organogenesis and embryo development, whole-body *Appl2*^{-/-} mice were generated by crossing *Appl2*^{L/L} mice to *EIIA-Cre* mice, followed by PCR-based genotyping of tail DNA (Fig. 1D). Homozygous *Appl2* knockout mice were found to be viable, and immunoblot analysis confirmed the loss of *Appl2* protein expression in tissues from various organs, for example, heart and liver, in *Appl2*^{-/-} mice (Fig. 1E).

***Appl2* is dispensable for embryonic development and reproduction**

Genotyping of litters from *Appl2*^{+/-} × *Appl2*^{+/-} mice revealed normal Mendelian ratios of genotype distributions, suggesting that loss of *Appl2* does not impact embryonic

development (Supplementary Fig. S1A). Moreover, *Appl2* loss did not impair reproductive function, given that similar litter sizes were observed among *Appl2*^{+/+} × *Appl2*^{+/+}, *Appl2*^{+/-} × *Appl2*^{+/-} and *Appl2*^{-/-} × *Appl2*^{-/-} matings (Supplementary Fig. S1B).

Dual loss of *Appl1* and *Appl2* does not impair organogenesis and reproductive function

To predict the tissues that might be adversely affected upon the co-deletion of both *Appl1/2* genes, we determined the abundance of *Appl1* and *Appl2* using real-time PCR (Supplementary Fig. S2). To further delineate the role of *Appl1* and *Appl2* in development, we set up a series of crosses to generate *Appl1*^{-/-};*Appl2*^{-/-} DKO mice. Unexpectedly,

genotyping of offspring from *App1* +/−;*App2* +/− × *App1* +/−;*App2* +/− crosses revealed normal Mendelian ratios (Fig. 2A). *App1*/*2* DKO mice showed grossly normal postnatal growth with slightly lower average body weight, which did not reach statistical significance (Fig. 2B). Moreover, *App1*/*App2* DKO mice have unimpaired reproductive function when compared to normal littermates (Fig. 2C).

Deficiency of *App1* and *App2* affects the physiology of erythrocytes, but not hematopoietic stem cell (HSC) differentiation

Complete blood counts (CBC) of 8-week-old mice revealed that deletion of *App1* and/or *App2* did not have an effect on the numbers and percentages of lymphocytes, monocytes, neutrophils, eosinophils, and basophils. However, hematocrit (HCT), mean corpuscular volume (MCV), and mean corpuscular hemoglobin concentration (MCHC) were slightly but significantly altered in *App1* −/−, *App2* −/− and *App1*/*App2* DKO mice, particularly in female mice. These changes were not severe enough to cause pernicious anemia, as WBC counts as well as the sizes of spleens and livers were normal (Table 2 and Supplementary Table S2).

***App1* proteins are not required for Pi3k-Akt signaling in thymic T-cell and other tissues**

We previously found that among all tissues tested, the greatest amount of interaction between *App1*/*2* and the

p110β subunit of Pi3k occurs in thymic T cells. Despite this, we report here that basal level of Akt activation is not altered in thymic T cells from DKO mice under normal husbandry conditions (Fig. 3A). Moreover, no consistent alteration of basal Akt activity was observed in tissues from stomach, liver or muscle among wild type (WT), *App1* KO, *App2* KO, and DKO mice (stomach shown in Fig. 3B, Supplementary Fig. S3).

Co-deletion of *App1* and *App2* does not affect T-cell development

Freshly isolated thymic T cells or spleen cells from WT and *App1*/*App2* DKO mice were subjected to flow cytometry analysis. CD4/CD8 and CD25/CD44 staining demonstrated that the total cell count of CD4/8 double positive (DP), CD4+, CD8+, and double negative (DN1, DN2, DN3, and DN4) do not differ significantly between the two genotypes (Fig. 4A and B). The total mature T-cell count in the spleen also was not changed in DKO mice (Fig. 4C and D). Moreover, we observed no significant change in the percentage of CD4+, CD8+ cells, CD25+ or CD44+ cells in DKO thymus (Fig. 4E and F). The proportion of TCRδ cells also was not appreciably changed in DKO thymus (Fig. 4G). In spleen, the T/B cell ratio in DKO mice did not differ significantly from that of WT mice (Fig. 4H). Moreover, CD4+, CD8+, or TCRδ+ populations also were not changed (Fig. 4I and J). Collectively, these findings suggest that *App1* and *App2* do not have a crucial role in T-cell development.

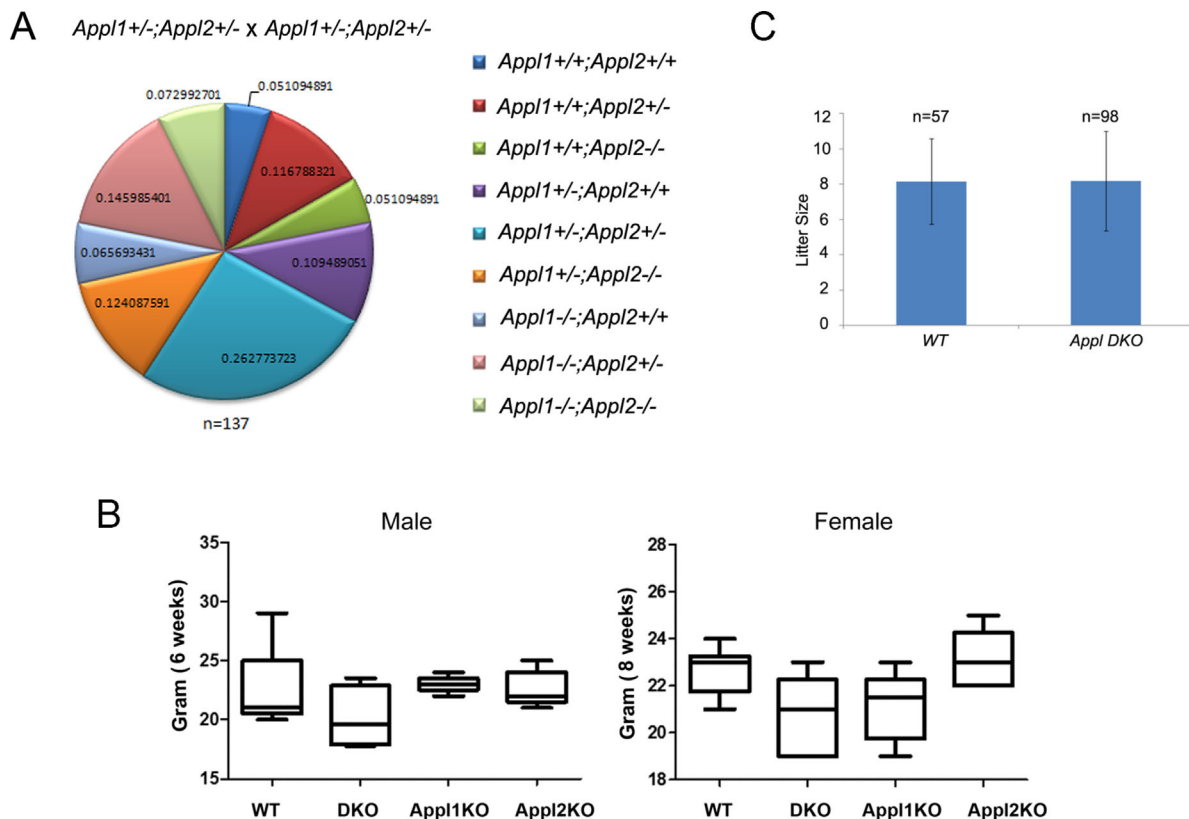


Fig. 2. *App1*/*App2* double-knockout (DKO) mice are viable and grossly normal. Normal Mendelian ratio of genotype distribution in litters from *App1* +/−;*App2* +/− × *App1* +/−;*App2* +/− matings (A). Box plots demonstrating that *App1* DKO mice show normal postnatal growth base and body weight at 6 weeks (males) and 8 weeks (females; B). Histogram showing similar average litter sizes arising in WT × WT and *App1* DKO × *App1* DKO matings (C).

TABLE 2. Complete blood counts from WT, *App1* KO, *App2* KO and DKO female mice

	WT	DKO	<i>App1</i> KO	<i>App2</i> KO
WBC (10 ⁹ /L)	7.75 ± 1.23	6.48 ± 1.71	8.17 ± 1.65	8.53 ± 2.51
LYM (10 ⁹ /L)	6.83 ± 0.89	5.47 ± 1.08	6.9 ± 1.34	7.18 ± 2.00
MON (10 ⁹ /L)	0.10 ± 0.05	0.21 ± 0.17	0.12 ± 0.06	0.09 ± 0.05
NEU (10 ⁹ /L)	0.81 ± 0.55	0.8 ± 0.48	1.16 ± 0.36	1.25 ± 0.65
LYM (%)	88.7 ± 4.88	85.3 ± 5.23	84.57 ± 2.75	84.58 ± 4.13
MON (%)	1.47 ± 0.69	3.00 ± 1.51	1.47 ± 0.65	1.25 ± 0.62
NEU (%)	9.8 ± 5.52	11.63 ± 3.81	13.93 ± 3.05	14.13 ± 4.07
RBC (10 ¹² /L)	11.14 ± 0.75	10.96 ± 0.23	10.94 ± 0.75	11.24 ± 0.46
HGB (g/dl)	16.17 ± 0.50	16.2 ± 0.69	16.57 ± 1.27	16.58 ± 0.40
HCT (%)	50.77 ± 2.40	56.84 ± 1.65**	54.68 ± 3.63*	57.88 ± 1.42***
MCV (ft)	46.00 ± 1.29	52.00 ± 1.00***	50.17 ± 3.71	51.75 ± 0.96****
MCH (pg)	14.63 ± 0.80	14.8 ± 0.60	15.12 ± 0.50	14.75 ± 0.41
MCHC (g/dl)	31.8 ± 1.42	28.53 ± 0.61**	30.33 ± 2.18	28.65 ± 0.44***
RDWc (%)	17.93 ± 0.57	19.13 ± 0.5*	20.02 ± 0.96***	18.55 ± 0.26*
PLT (10 ⁹ /L)	518 ± 88.01	533.67 ± 50.5	547.17 ± 82.53	742.25 ± 90.7*
PCT (%)	0.32 ± 0.04	0.40 ± 0.03*	0.43 ± 0.08	0.63 ± 0.11***
MPV (ft)	6.3 ± 0.68	7.57 ± 0.21**	7.77 ± 0.38****	8.5 ± 0.63****
PDWc (%)	30.13 ± 2.33	34.27 ± 1.81	37.78 ± 2.02**	37.05 ± 2.12****

Note: compared to WT mice.

**P* < 0.05.

***P* < 0.01.

****P* < 0.005.

*****P* < 0.001.

App1 and *App2* potentiate HGF-induced Pi3k-Akt signaling and motility in primary MEFs

We previously showed that EGF, insulin or serum trigger robust Akt activation in serum-starved MEFs independent of *App1* status, whereas *App1* is required for moderate Akt activation triggered by HGF (Tan et al., 2010b). Here, we further demonstrate that *App2* is not required for robust activation of Akt by EGF or serum. MEFs generated from E13.5-day-old embryos were harvested and used in early passages. MEFs from *App2* KO or *App1/2* DKO mice showed no appreciable difference in the level of Akt activation upon stimulation with 10% serum or 20 ng/ml EGF for 5–40 min (Fig. 5A). Interestingly, *App1* KO, *App2* KO, and especially *App1/2* DKO MEFs showed consistently decreased Akt activation upon stimulation with HGF (Fig. 5B). Further study revealed that loss of *App1* proteins results in reduced HGF-triggered transmembrane migration (Fig. 5C,D and Supplementary Fig. S4A) and decreased movement in a

wound-healing assay (Supplementary Fig. S4B). Additionally, *App1*-deficient MEFs showed markedly decreased HGF-triggered invasion in a matrigel assay, indicating that loss of *App1* proteins impairs cell invasion following stimulation with HGF (Fig. 5E and F). However, no difference in invasive ability was observed between WT and *App1/2* knockout cells in response to EGF (Supplementary Fig. S4C and D), presumably due to unaffected EGF-Akt signaling in *App1* KO cells.

Discussion

Recent in vitro studies on *App1* and *App2* by several labs, using RNAi or expression constructs, have generated paradoxical results (Miaczynska et al., 2004; Saito et al., 2007; Tu et al., 2011; Broussard et al., 2012; Yeo et al., 2015). Unbiased genetic evidence is, therefore, needed to better understand the function of *App1* proteins. To address this need, in vivo studies using gene knockout strategies have been applied. We previously reported that *App1* knockout mice have normal embryonic development and reproduction, with generally normal Akt signaling in various tissues tested, and we raised the possibility that *App1* proteins may substitute for each other during development and in cell signaling (Tan et al., 2010a,b). As *App2* knockout mice were not available at that time to test this idea in vivo, we used an RNAi approach to knock down *App2* in *App1*−/− MEFs. We found that *App1* and *App2* are functionally redundant and dispensable for cell survival under normal cell culture conditions. In the present study with *App2*−/− mice, we found that *App2* is dispensable for development and reproduction. Moreover, we discovered that *App1;App2* DKO mice are viable and grossly normal without marked defects in Akt signaling in vivo. We previously reported that *App1* and *App2* each interacts strongly with the p110 subunit of Pi3k in thymic T cells in vivo (Tan et al., 2010a). However, this interaction does not appear to be required for basal level of Pi3k-Akt signaling in thymic T cells; moreover, *App1*−/−, *App2*−/−, and DKO mice each demonstrated normal T-cell development. Altogether, these findings strongly suggest that *App1* and *App2* genes are functionally redundant during organogenesis and postnatal growth under normal conditions. Furthermore, our studies on MEFs from these mice revealed that only under certain conditions, specifically upon stimulation with HGF, do *App1* and *App2* regulate Akt activity and cell migration/invasion.

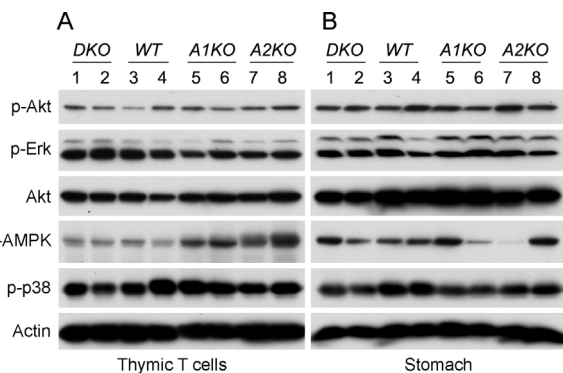


Fig. 3. *App1;App2* DKO mice have unaltered Pi3k signaling in vivo. Tissues from thymic T cells (A) and stomach (B) were subjected to immunoblotting using antibodies against the indicated proteins. Levels of phospho-Akt, phospho-Erk, phospho-p38, and phospho-AMPK were compared among the four genotypes. A1KO = *App1* KO mice; A2KO = *App2* KO mice.

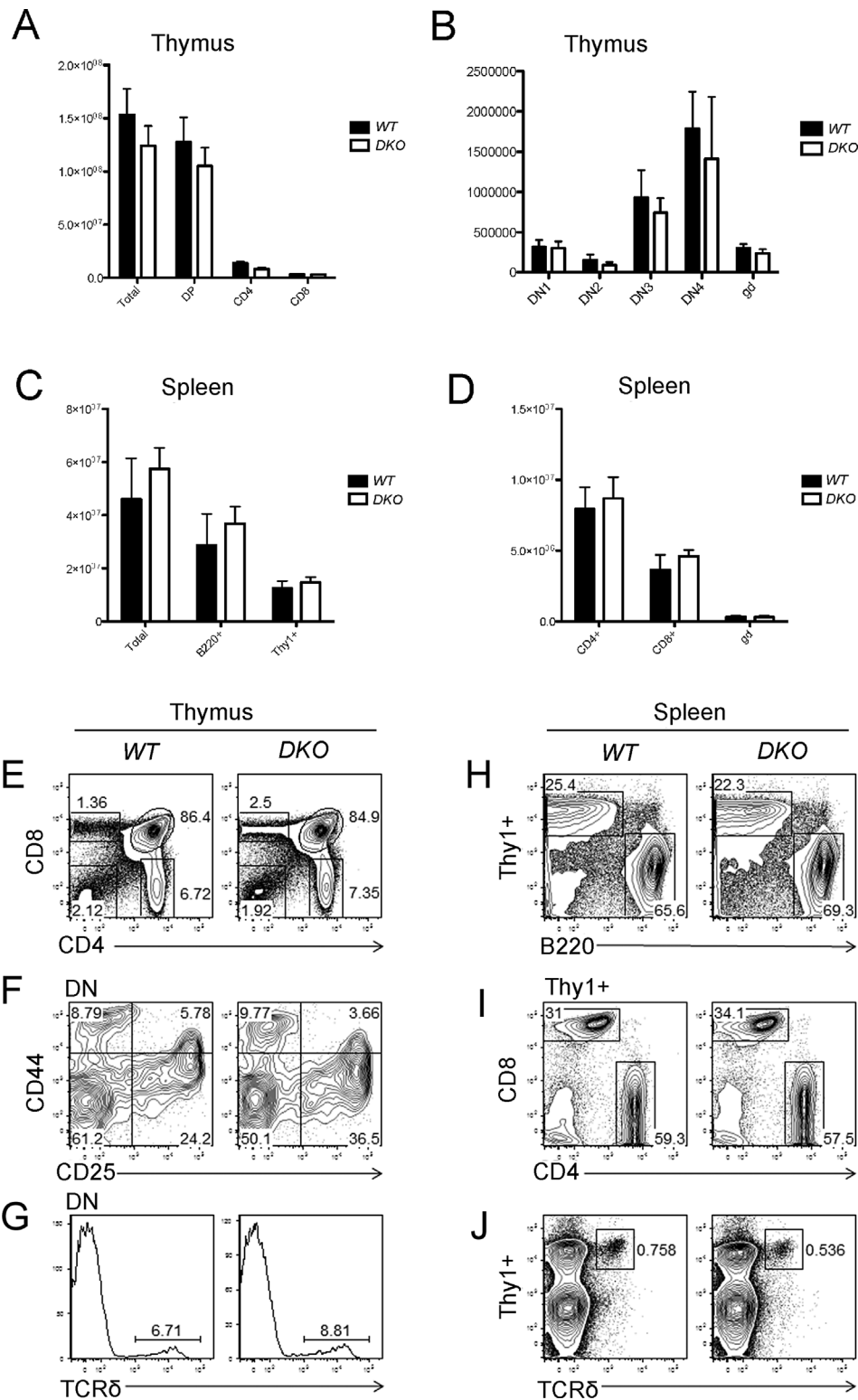


Fig. 4. Co-deletion of *App1* and *App2* do not affect T-cell development. WT and *App1* DKO mice at 6 weeks of age were sacrificed to collect thymus (A,B) and spleen cells (C,D). Cells were stained with fluorescence-labeled anti-CD4, CD8, CD44, CD25, Thy1, and B220 antibodies, and then counted using multicolor flow cytometry. (A) CD4⁺, CD8⁺, and CD4⁺CD8⁺ (DP) cells in thymus. (B) Distribution of various stages of CD4/CD8 double-negative (DN) cells in thymus of WT and *App1* DKO mice. gd = $\gamma\delta$ T cells. (C) Thy1⁺ and B220⁺ population in spleen. (D) Mature CD4⁺ and CD8⁺ T-cells in spleen. (E) Percentages of CD4⁺, CD8⁺ and CD4⁺CD8⁺ and CD4⁻CD8⁻ populations in thymus of WT and DKO mice. (F) Distribution of CD44⁺, CD25⁺, CD44⁻CD25⁺, and CD44⁻CD25⁻ cells. (G) TCR δ population in thymus cells from WT and DKO mice. (H,I,J) Percentages of Thy1⁺ and B220⁺ populations, mature CD4⁺ or CD8⁺ T-cells, and TCR δ T cells in spleen, respectively.

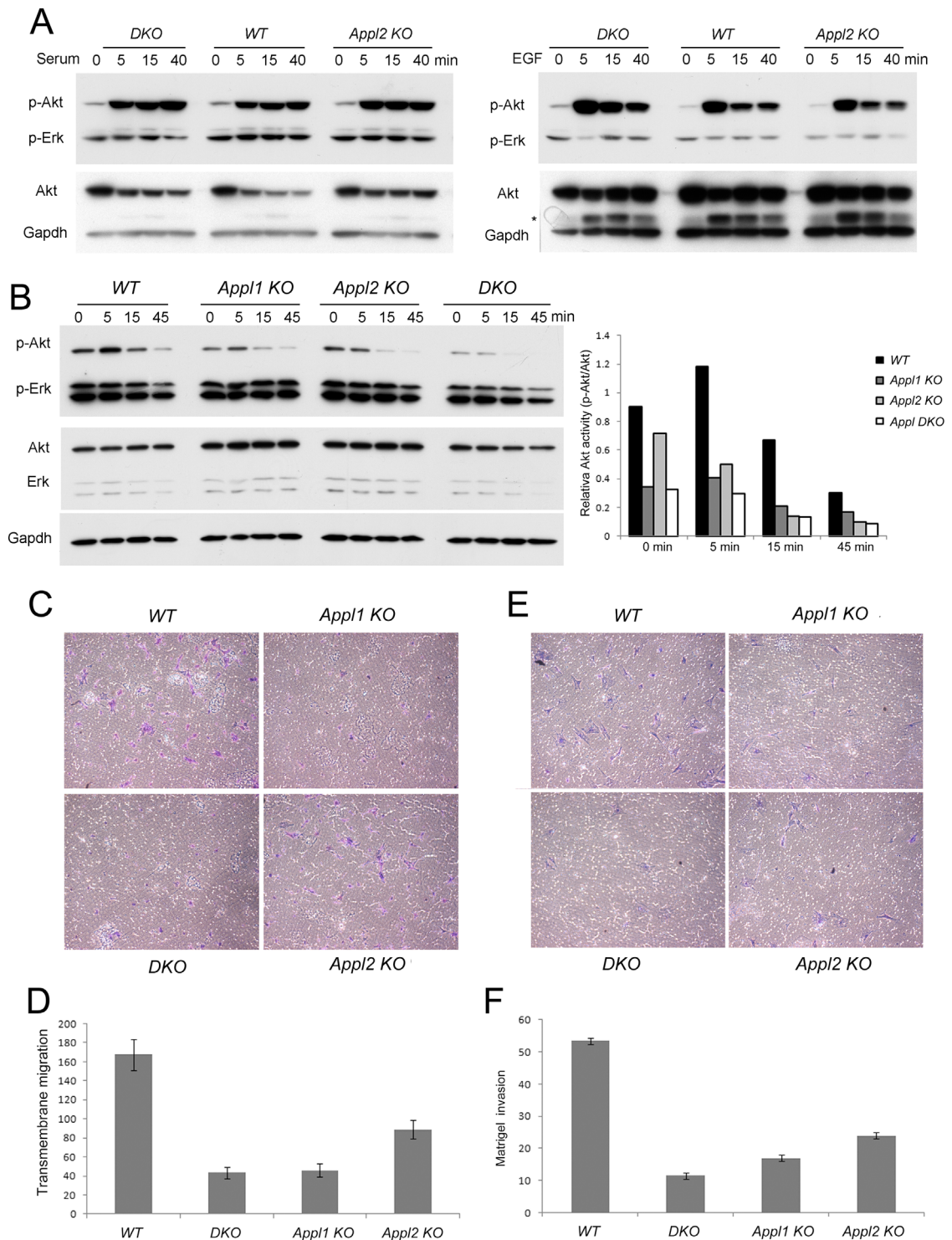


Fig. 5. *Appl* proteins are required for HGF-induced, but not FBS- or EGF-induced, Akt activation and migration in MEFs. (A) Primary MEFs from WT, *Appl2*^{-/-} and *Appl* DKO embryos were seeded overnight, starved with serum-free media, and then stimulated with 10% FBS (upper panel) or 20 ng/ml EGF (lower panel) for the indicated times. (B) MEFs from WT, *Appl1*^{-/-}, *Appl2*^{-/-}, and *Appl* DKO embryos were starved and treated with 50 ng/ml HGF. The histogram depicts the relative densitometry levels of phosphorylated Akt normalized against total Akt protein levels. (C,D) MEFs were seeded on 8.0 μ M PET inserts with DMEM plus 0.1% FBS at the top chamber. The lower chamber was filled with 100 ng/ml HGF in DMEM plus 0.1% FBS. Cells migrating to the other side of the membrane were fixed, stained and counted after 6 h. (E, F) Results of invasion assay using Matrigel invasion chambers, with cells counted 48 h after seeding. Migrated or invaded cell numbers were counted and normalized against the seeding cell numbers.

AKT signal transduction pathway regulates many cellular survival mechanisms including cell cycle progression, metabolism, anti-apoptosis, invasion, and metastasis (Vogiatzi and Giordano, 2007). Many growth factors can activate AKT signaling including EGF, Insulin, IGF, FGF and HGF, etc., (Burgering and Coffey, 1995; Magun et al., 1996; Sanchez-Margalet, 2000; Forough et al., 2006). HGF-Met signaling has been implicated in tumor growth, invasion, and metastasis, partially via Akt (Shinomiya et al., 2004). Previously, we reported that only a very small percentage of all Akt protein binds to Appl1 or Appl2 protein in MEFs. This may explain why only a weak mitogen, such as HGF, not a stronger mitogen, such as EGF, requires Appl1 protein to activate Akt in MEFs (Tan et al., 2010b). In the present study, we found that this is also the case with *Appl2*^{-/-} MEFs and *Appl* DKO MEFs. When compared MEFs from *WT* mice, *Appl*-deficient MEFs exhibit impaired ability to migrate or invade Matrigel in response to HGF stimulation *in vitro*. Interesting, basal level of Akt activation in the liver is not altered in *Appl* knockout mice under normal conditions. This may be because c-Met is not required for normal liver function but is essential for regeneration after liver injury (Huh et al., 2004). Therefore, we speculate that *Appl* knockout mice might exhibit defects in liver regeneration after injury. Moreover, mutation of HGF results in deafness in mice (Schultz et al., 2009). Future neurological studies should be performed in *Appl* knockout mice to assess hearing loss. With regard to cancer, loss of HGF/c-Met signaling accelerates N-nitrosodiethylamine-induced hepatocarcinogenesis (Takami et al., 2007). Given our group's longstanding interest in cancer research, we intend to carry out similar studies with *Appl1/2*-null mice to test if Appl proteins have a tumor suppressor function, and if such a potential role were associated with HGF signaling during hepatocarcinogenesis.

Appl1 and Appl2 proteins possess BAR, PH, and PTP domains. BAR domains can dimerize and interact with BAR-PH domains. The BAR, PH, and PTP motifs are each capable of binding phospholipids and possess membrane binding properties (Li et al., 2007). BAR domain proteins bind to small GTPases to induce membrane curvature (Habermann, 2004). Moreover, Appl1 and Appl2 can form homo- or hetero-oligomers via their BAR domains. Appl protein can recruit Rab5 to moving membrane structures (Chial et al., 2008). In this study, we discovered that *Appl* knockout mice, particularly *Appl2*-null and *DKO* mice, exhibit altered red blood cell physiology. These cells generally were larger and had a more irregular shape than erythrocytes from *WT* mice. Thus, we speculate that Appl proteins normally may bind to the cellular membrane of erythrocytes and facilitate the maintenance of the biconcave disk.

Finally, the finding that *Appl*-deficient mice are grossly normal with regard to reproductive potential is intriguing, given that prior work demonstrated a potential link between the follicle-stimulating hormone receptor (FSHR) and APPL1 (Nechamen et al., 2004). In this earlier *in vitro* work, FSHR was shown to interact with APPL1, and FOXO1a, a downstream effector in the PI3K pathway tightly connected with expression of proapoptotic genes, was found to be rapidly inactivated when FSHR-expressing human cells were treated with FSH. Thus, a possible link between FSH and PI3K/Akt signaling was proposed as a survival mechanism whereby FSH selects the dominant follicle to survive. However, our current work with Appl knockout models revealed no obvious changes with regard to fertility.

Acknowledgments

We thank the Flow Cytometry and Laboratory Animal Facilities at Fox Chase Cancer Center for assistance. This

work was supported by the NIH grants (NCI-CA77429, CA083638 and CA06927 to J.R.T., and NIDDK-DK102965 to L.Q.D.) and by American Diabetes Association Award (grant # 7-13-BS-043 to L.Q.D.), an appropriation from the Commonwealth of Pennsylvania, and a CCSG Pilot Project from Fox Chase Cancer Center.

Literature Cited

- Altomare DA, Lyons GE, Mitsuuchi Y, Cheng JQ, Testa JR. 1998. Akt2 mRNA is highly expressed in embryonic brown fat and the AKT2 kinase is activated by insulin. *Oncogene* 16:2407–2411.
- Broussard JA, Lin WH, Majumdar D, Anderson B, Eason B, Brown CM, Webb DJ. 2012. The endosomal adaptor protein APPL1 impairs the turnover of leading edge adhesions to regulate cell migration. *Mol Biol Cell* 23:1486–1499.
- Burgering BM, Coffey PJ. 1995. Protein kinase B (c-Akt) in phosphatidylinositol-3-OH kinase signal transduction. *Nature* 376:599–602.
- Cheng KK, Lam KS, Wu D, Wang Y, Sweeney G, Hoo RL, Zhang J, Xu A. 2012. APPL1 potentiates insulin secretion in pancreatic beta cells by enhancing protein kinase Akt-dependent expression of SNARE proteins in mice. *Proc Natl Acad Sci USA* 109:8919–8924.
- Chial HJ, Wu R, Ustach CV, McPhail LC, Mobley WC, Chen YQ. 2008. Membrane targeting by APPL1 and APP L2: Dynamic scaffolds that oligomerize and bind phosphoinositides. *Traffic* 9:215–229.
- Erdmann KS, Mao Y, McCrean HJ, Zoncu R, Lee S, Paradise S, Modregger J, Biemesderfer D, Toomre D, De Camilli P. 2007. A role of the Lowe syndrome protein OCRL in early steps of the endocytic pathway. *Dev Cell* 13:377–390.
- Forough R, Weylie B, Collins C, Parker JL, Zhu J, Barhouri R, Watson DK. 2006. Transcription factor Ets-1 regulates fibroblast growth factor-1-mediated angiogenesis *in vivo*: Role of Ets-1 in the regulation of the PI3K/AKT/MMP-1 pathway. *J Vasc Res* 43:327–337.
- Habermann B. 2004. The BAR-domain family of proteins: A case of bending and binding? *EMBO Rep* 5:250–255.
- Hennig J, McShane MP, Cordes N, Eke I. 2014. APPL proteins modulate DNA repair and radiation survival of pancreatic carcinoma cells by regulating ATM. *Cell Death Disease* 5:e1199.
- Huh CG, Factor VM, Sanchez A, Uchida K, Conner EA, Thorgeirsson SS. 2004. Hepatocyte growth factor/c-met signaling pathway is required for efficient liver regeneration and repair. *Proc Natl Acad Sci USA* 101:4477–4482.
- Li J, Mao X, Dong LQ, Liu F, Tong L. 2007. Crystal structures of the BAR-PH and PTB domains of human APPL1. *Structure* 15:525–533.
- Lin DC, Quevedo C, Brewer NE, Bell A, Testa JR, Grimes ML, Miller FD, Kaplan DR. 2006. APPL1 associates with TrkA and GIPC1 and is required for nerve growth factor-mediated signal transduction. *Mol Cell Biol* 26:8928–8941.
- Magun R, Burgering BM, Coffey PJ, Pardasani D, Lin Y, Chabot J, Sorisky A. 1996. Expression of a constitutively activated form of protein kinase B (c-Akt) in 3T3-L1 preadipose cells causes spontaneous differentiation. *Endocrinology* 137:3590–3593.
- Mao X, Kikani CK, Riojas RA, Langlais P, Wang L, Ramos FJ, Fang Q, Christ-Roberts CY, Hong JY, Kim RY, Liu F, Dong LQ. 2006. APPL1 binds to adiponectin receptors and mediates adiponectin signalling and function. *Nat Cell Biol* 8:516–523.
- Miaczynska M, Christoforidis S, Giner A, Shevchenko A, Uttenweiler-Joseph S, Habermann B, Wilim M, Parton RG, Zerial M. 2004. APPL proteins link Rab5 to nuclear signal transduction via an endosomal compartment. *Cell* 116:445–456.
- Mitsuuchi Y, Johnson SW, Sonoda G, Tanno S, Golemis EA, Testa JR. 1999. Identification of a chromosome 3p14.3-21.1 gene, APPL, encoding an adaptor molecule that interacts with the oncoprotein-serine/threonine kinase A KT2. *Oncogene* 18:4891–4898.
- Nechamen CA, Thomas RM, Cohen BD, Acevedo G, Poulikakos PI, Testa JR, Dias JA. 2004. Human follicle-stimulating hormone (FSH) receptor interacts with the adaptor protein APPL1 in HEK 293 cells: Potential involvement of the PI3K pathway in FSH signaling. *Biol Reprod* 71:629–636.
- Pilecka I, Sadowski L, Kalaidzidis Y, Miaczynska M. 2011. Recruitment of APPL1 to ubiquitin-rich aggregates in response to proteasomal impairment. *Exp Cell Res* 317:1093–1107.
- Ryu J, Galan AK, Xin X, Dong F, Abdul-Ghani MA, Zhou L, Wang C, Li C, Holmes BM, Sloane LB, Austad SN, Guo S, Musi N, DeFronzo RA, Deng C, White MF, Liu F, Dong LQ. 2014. APPL1 potentiates insulin sensitivity by facilitating the binding of IRS1/2 to the insulin receptor. *Cell Rep* 7:1227–1238.
- Saito T, Jones CC, Huang S, Czech MP, Pilch PF. 2007. The interaction of Akt with APPL1 is required for insulin-stimulated Glut4 translocation. *J Biol Chem* 282:32280–32287.
- Sanchez-Margalet V. 2000. Stimulation of glycogen synthesis by insulin requires S6 kinase and phosphatidylinositol-3-kinase in HTC-IR cells. *J Cell Physiol* 182:182–188.
- Schenck A, Goto-Silva L, Collinet C, Rhinn M, Giner A, Habermann B, Brand M, Zerial M. 2008. The endosomal protein Appl1 mediates Akt substrate specificity and cell survival in vertebrate development. *Cell* 133:486–497.
- Schultz JM, Khan SN, Ahmed ZM, Riazuddin S, Waryah AM, Chhatre D, Starost MF, Ploplis B, Buckley S, Velasquez D, Kabra M, Lee K, Hassan MJ, Ali G, Ansar M, Ghosh M, Wilcox ER, Ahmad W, Merlino G, Leal SM, Riazuddin S, Friedman TB, Morell RJ. 2009. Noncoding mutations of HGF are associated with nonsyndromic hearing loss, DF NB39. *Am J Hum Genet* 85:25–39.
- Shinomiya N, Gao CF, Xie Q, Gustafson M, Waters DJ, Zhang YW, Vande Woude GF. 2004. RNA interference reveals that ligand-independent met activity is required for tumor cell signaling and survival. *Cancer Res* 64:7962–7970.
- Takami T, Kaposi-Novak P, Uchida K, Gomez-Quiroz LE, Conner EA, Factor VM, Thorgeirsson SS. 2007. Loss of hepatocyte growth factor/c-Met signaling pathway accelerates early stages of N-nitrosodiethylamine induced hepatocarcinogenesis. *Cancer Res* 67:9844–9851.
- Tan Y, You H, Coffey PJ, Wiest DL, Testa JR. 2010a. Appl1 is dispensable for Akt signaling *in vivo* and mouse T-cell development. *Genesis* 48:531–539.
- Tan Y, You H, Wu C, Altomare DA, Testa JR. 2010b. Appl1 is dispensable for mouse development, and loss of Appl1 has growth factor-selective effects on Akt signaling in murine embryonic fibroblasts. *J Biol Chem* 285:6377–6389.

- Tu Q, Zhang J, Dong LQ, Saunders E, Luo E, Tang J, Chen J. 2011. Adiponectin inhibits osteoclastogenesis and bone resorption via APPL1-mediated suppression of Akt1. *J Biol Chem* 286:12542–12553.
- Vogiatzi P, Giordano A. 2007. Following the tracks of AKT1 gene. *Cancer Biol Ther* 6:1521–1524.
- Wang C, Xin X, Xiang R, Ramos FJ, Liu M, Lee HJ, Chen H, Mao X, Kikani CK, Liu F, Dong LQ. 2009. Yin-Yang regulation of adiponectin signaling by APPL isoforms in muscle cells. *J Biol Chem* 284:31608–31615.
- Wang C, Li X, Mu K, Li L, Wang S, Zhu Y, Zhang M, Ryu J, Xie Z, Shi D, Zhang WJ, Dong LQ, Jia W. 2013. Deficiency of APPL1 in mice impairs glucose-stimulated insulin secretion through inhibition of pancreatic beta cell mitochondrial function. *Diabetologia* 56:1999–2009.
- Wen L, Yang Y, Wang Y, Xu A, Wu D, Chen Y. 2010. Appl1 is essential for the survival of *Xenopus* pancreas, duodenum, and stomach progenitor cells. *Dev Dyn* 239:2198–2207.
- Yeo JC, Wall AA, Luo L, Stow JL. 2015. Rab31 and APPL2 enhance FcγR-mediated phagocytosis through PI3K/Akt signaling in macrophages. *Mol Biol Cell* 26:952–965.
- Zhu G, Chen J, Liu J, Brunzelle JS, Huang B, Wakeham N, Terzyan S, Li X, Rao Z, Li G, Zhang XC. 2007. Structure of the APPL1 BAR-PH domain and characterization of its interaction with Rab5. *EMBO J* 26:3484–3493.

Supporting Information

Additional supporting information may be found in the online version of this article at the publisher's web-site.